SAND2020-2415C

Symposium: Advancement of Optical Methods in Experimental Mechanics

Solid Cylinder Torsion Experiment for Large Shear Deformation

H. Jin[1], W-Y. Lu [1], J.W. Foulk[1], J. Ostien[1], S.L. Kramer[2], A. Jones[2]
[1] Sandia National Laboratories, Livermore, CA 94551
[2] Sandia National Laboratories, Albuquerque, NM 87122

Abstract

Using a thin-walled tube torsion test to characterize a material's shear response is a well-known technique; however, the thin walled specimen tends to buckle before reaching large shear deformation and failure. An alternative technique is the surface stress method [1, 2], which derives a shear stress-strain curve from the torque-twist relationship of a solid cylindrical bar; however this method has rarely been considered in the literature, possibly due to the complexity of the analysis and experimental issues such as twist measurement and specimen uniformity. Even with the difficulties involved, the solid bar torsion test has become very attractive because the stable deformation uniquely allows us to control and explore very large shear deformation up to failure. In this investigation, solid bar torsion experiments were conducted to study large shear deformation of two common engineering materials, Al6061-T6 and SS304L, which have distinctive hardening behaviors. Modern 3D DIC methods were applied to make deformation measurements. The twist angle of the specimen could be significantly large, which posed challenges to the DIC analysis. A method was developed to make the necessary measurements successful. Solid bar specimens were twisted to failure; engineering shear strains at failure were all greater than 2. Shear stress-strain curves of Al6061-T6 and SS304L were obtained.

Keywords: ductile failure, large deformation, digital image correlation, shear stress-strain curve, torsion, Al6061-T6, SS304

1. Background of Solid Cylinder Torsion

The theory of using solid bar torsion data for shear stress-strain relations was developed in 1950. Consider a solid cylinder under torsion and a surface element shown in Figure 1, where *x*, *y*, and z are hoop, axial and radial directions, respectively. The well-known solution by Nadai [1] is

$$\tau = \frac{1}{2\pi {r_o}^3}\left(\omega \frac{dT}{d\omega} + 3T\right), \tag{1}$$

where τ is the surface shear stress, r_o is the initial radius of the cylinder, *T* is the torque, and ω is the twist per unit length. The normal strain $e_x = e_y = e_z = 0$ is assumed, i.e. the dimension of the circular cylinder during torsion is always the same as the original, $r = r_o$. The shear strain is

$$\gamma = r_o \omega. \tag{2}$$

Equations (1) and (2) give the engineering shear stress-stain curve.

By adding axial elongation and radius change of the cylinder at large strain torsion, the solution was modified by Wu et al in 1992 [2]

$$\tau_t = \frac{1}{2\pi {r_o}^3}\left(\omega \frac{dT}{d\omega} + 3T\right)\left(\frac{1}{1-\frac{1}{2}\left(3e_y + \omega \frac{de_y}{d\omega}\right)}\right), \tag{3}$$

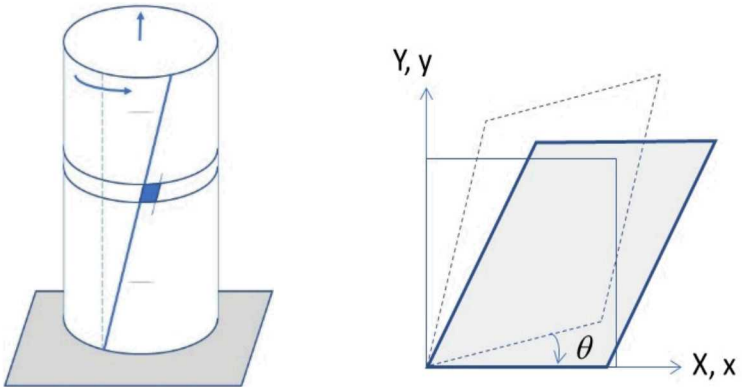

Figure 1. A circular cylinder under axial-torsional deformation.

here axial strain e_y is a function of ω, and material incompressibility is assumed.

$$e_x = e_z = -\frac{1}{2}e_y \tag{4}$$

We note that both incompressibility and additional simplification stem from the assumption that the shear strain is potentially large but the axial extension and radial contraction are small. The shear strain is

$$\gamma_t = r\omega = r_o(1 + e_x)\omega, \tag{5}$$

Since the analysis is based on the deformed geometry, Equations (3) and (5) yield the true stress-strain curve for small volumetric deformations.

Although these solutions have been available for decades, experimental studies of shear characterization using solid bar torsion experiments are very limited. Only a handful tests can be found in literature. In 1991, Lyon [3] showed reasonable agreement between shear stress-strain curves obtained from thin-wall tubes and solid cylinders made of epoxy. Nadai's surface method was applied for the solid cylinder specimen. After yielding, the shear stresses obtained from thin-wall tubular specimens were higher by at most 10%. The difference was attributed to the friction between the tube and the lubricated rigid insert, which was fitted in the tube to prevent it from buckling. The maximum shear strain reached was less than 25%.

About the same time, Wu et al [2] compared the shear stress-strain curves of high purity cast aluminum from torsion tests of solid cylinders and tubular specimens of various wall thickness. The twist and elongation of the gage section was carefully measured by an extensometer. Both Nadai's solution and Wu's modification were illustrated. Take the solid cylinder data at large shear strain γ =130% for instance, the axial strain $e_y \approx 0.012$, and the value of $de_y/d\gamma \approx 0.015$. The maximum difference between these two approaches was estimated to be about 3.5%. The results of the solid cylinder and tubular specimen agreed well if Wu's modification was used. Wu [4] performed more tests and discussed testing issues and specimen geometries. Deformation uniformity was critical for the approach. A well-controlled homogeneous aluminum, special for the experiment, was used. Maximum shear strain reached was about 200%. A long gage section was recommended to minimize the effect of shoulders.

More recently, Kingsbury [5] used solid bars to obtain shear stress-stain curves of a crosslinked PMMA at three different shear rates utilizing Wu's modification. Shear stress-strain curves were established up to a very large shear strain $\gamma_t \approx 200\%$.

Shear failure was not discussed in above-mentioned investigations. Papasidero et al [6]

did *in situ* torsion tests in SEM on cylindrical specimens of 36NiCrMo16 steel. Tests were stopped at intervals to monitor strain and damage evolution. The micro-grids method was used for an approximate evaluation of the engineering shear strain and axial strain. Out of surface displacement prevented the application of digital image correlation (DIC) method.

2. New Analysis Approach for Large Strains in Solid Cylinder Torsion

In this investigation, a new approach is developed to overcome the diagnostic difficulties experienced for the solid bar torsion setup. The idea is to adopt a new reference configuration periodically so that "incremental" deformation can always be evaluated over an adequate surface area. To accomplish this experimentally, the whole gage section needs to be painted with DIC speckles and the reference configuration needs to be reset no more than every 60° of rotation. It is necessary to map the "incremental" results back to the original reference configuration and then evaluate parameters that involved in the stress calculation, Equation (1) or (3).

To convert a set of DIC data, which is based on a deformed reference configuration, to the initial undeformed reference configuration can be accomplished by considering the deformation gradient *F*. When a cylinder is under axial-torsional deformation, as shown in Fig. 1, the deformation gradient of a surface point and its relationship with engineering strains can be approximated by

$$\boldsymbol{F} = \begin{bmatrix} p & k & 0 \\ 0 & q & 0 \\ 0 & 0 & s \end{bmatrix} = \begin{bmatrix} 1+e_x & \gamma & 0 \\ 0 & 1+e_y & 0 \\ 0 & 0 & 1+e_z \end{bmatrix}, \tag{6}$$

where y is along the cylinder axis, z is the radial direction, x is tangent to the surface and perpendicular to y and z.

Suppose the images of the speckled sample for 3D DIC analysis are acquired by a pair of cameras at a constant rate throughout the torsion experiment till failure. The sequential stage number identifies the deformation where images and data are taken. At stage i, the deformation is described by $d\boldsymbol{x}_i = \boldsymbol{F_i} d\boldsymbol{X}_o$, where X_o is the undeformed reference configuration and

$$\boldsymbol{F_i} = \begin{bmatrix} p_i & k_i & 0 \\ 0 & q_i & 0 \\ 0 & 0 & s_i \end{bmatrix}. \tag{7}$$

When the measurable area becomes small, it is necessary to make stage *I* be the new reference configuration $X_I = x_I$. For measurement stages $i > I$, the deformation $d\boldsymbol{x}_i = \boldsymbol{F_i}' d\boldsymbol{X}_I$ is the "incremental" deformation gradient with respect to reference stage *I*. The total deformation gradient $\boldsymbol{F_i}$ is a multiplicative decomposition of the incremental deformation gradient $\boldsymbol{F_i}'$ and the initial deformation gradient $\boldsymbol{F_I}$. We find

$$d\boldsymbol{x}_i = \boldsymbol{F_i}' d\boldsymbol{X}_I = \boldsymbol{F_i}' \boldsymbol{F_I} d\boldsymbol{X}_o = \boldsymbol{F_i} d\boldsymbol{X}_o, \tag{8}$$

and

$$\boldsymbol{F_i} = \boldsymbol{F_i}' \boldsymbol{F_I} = \begin{bmatrix} p_i' & k_i' & 0 \\ 0 & q_i' & 0 \\ 0 & 0 & s_i' \end{bmatrix} \begin{bmatrix} p_I & k_I & 0 \\ 0 & q_I & 0 \\ 0 & 0 & s_I \end{bmatrix} = \begin{bmatrix} p_i' p_I & p_i' k_I + k_i' q_I & 0 \\ 0 & q_i' q_I & 0 \\ 0 & 0 & s_i' s_I \end{bmatrix}. \tag{9}$$

If all normal engineering strains are zero, i.e. p=q=s=1, then the shear strain transformation is linear,

$$k_i = k_I + k_i'. \tag{10}$$

Notice that reference configuration *I* does not have the same physical specimen surface as the original reference configuration. Some portion of specimen has rotated out of, or into, the view

of the cameras. Not every point on the deformed reference configuration has a corresponding point on the original reference configuration. With very large rotation it is not possible to track the deformation field of the whole gage section with only one pair of cameras that has a fixed view. Fortunately, for stress and strain evaluation, only one deformation gradient is needed for each stage. Field information of the stage is not required. So instead of working with the deformation field, the averaged deformation gradient of an area of interest (AOI) is applied in Equation (9).

If the torsional deformation is axisymmetric, the averaged values over AOI will be consistent regardless of two reference configurations having different material points. In solid bar torsion analysis [1, 2], axisymmetric deformation is already a basic assumption. Using the averaged value does not introduce additional restrictions. We could utilize the incremental deformation field from DIC analysis to define AOI and to verify the deformation is axisymmetric.

3. Solid Cylinder Torsion Experiments

This experimental investigation included two engineering materials of interest: one was a 4-inch thick plate of certified Al6061-T6 and the other was a 7-inch diameter cylinder of SS304L-VAR. Al6061-T6 has little strain hardening. The curve is relatively flat after yielding. For SS304, the ultimate strength is more than the double of its initial yield stress.

Figure 2 shows the torsion test setup, consisting of a hydraulic axial-torsional testing system with capacities of $\pm$100 mm displacement and $\pm$140^o rotation. The system load cell is rated at $\pm$15 kN force and $\pm$150 N-m torque. It is equipped with a pair of hydraulic grips for quick installing and releasing specimens. During this pure shear test, the axial channel was under force control, which was kept at zero force *F=0*. The torsion channel was under rotation control. The shear loading-unloading program was set to rotate the actuator for a predetermined range, e.g., from actuator angular position Ω_a = -140^o to 140^o. If the specimen did not fail, the torque was unloaded to zero at the end of the program. At zero torque, the operator manually released one of the hydraulic grip which is typically on the actuator side, returned the actuator to the starting angular position, regripped the specimen, and restarted the program for another loading-unloading cycle. The process was repeated until specimen failed.

Parameters such as torque, force, rotation and displacement of the actuator were also acquired. Frame and data acquisitions were synchronized.

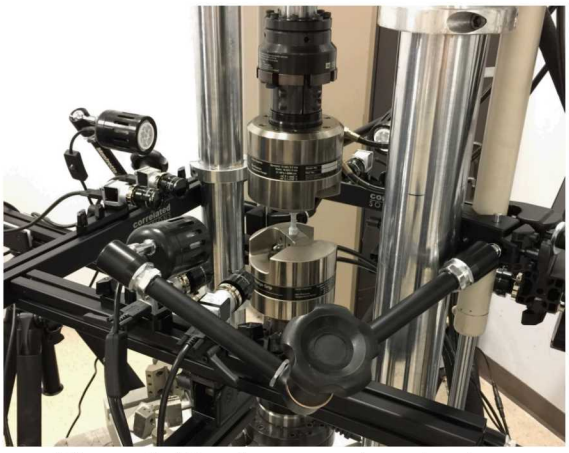

Figure 2. Torsion experiment setup.

Figure 2 shows the torsion test setup, consisting of a hydraulic axial-torsional testing

system with capacities of ±100 mm displacement and ±140° rotation. The system load cell is rated at ±15 kN force and ±150 N-m torque. It is equipped with a pair of hydraulic grips for quick installing and releasing specimens. During this pure shear test, the axial channel was under force control, which was kept at zero force *F=0*. The torsion channel was under rotation control. The shear loading-unloading program was set to rotate the actuator for a predetermined range, e.g., from actuator angular position Ω_a = -140° to 140°. If the specimen did not fail, the torque was unloaded to zero at the end of the program. At zero torque, the operator manually released one of the hydraulic grip which is typically on the actuator side, returned the actuator to the starting angular position, regripped the specimen, and restarted the program for another loading-unloading cycle. The process was repeated until specimen failed. Parameters such as torque, force, rotation and displacement of the actuator were also acquired. Frame and data acquisitions were synchronized.

Figure 3 shows the torque-rotation ($T - \Omega$) curves of three Al specimens. Specimen TOR_RD_1 failed at a total rotation of Ω = 340°, including one unloading-reloading at 280°; Specimens TOR_RD_2 and 3 failed at Ω = 255° and 265°, respectively, before unloading happened.

The torsion test of SS304L-VAR was basically the same as Al6061-T6 described above. The SS304L-VR specimens were cored from different radial distances from the center of a 190 mm (7.5") diameter cylinder. The radii of Ring1, Ring2 and Ring3 were about 73 mm, 63 mm and 28 mm, respectively. As shown in Figure 4(a) of torque-rotation curves, these specimens went through a very large rotation before failure, about 1,200 degrees. Based on Equations (1) or (3), the surface shear stress was calculated. The shear stress-strain curves are plotted in Fig. 4(b). The failure engineering shear strain is $\gamma \approx 4$. The difference in the results using the Nadai and Wu's theory is clearly shown in stainless steel with large localized strain where the change of diameter can not be neglected.

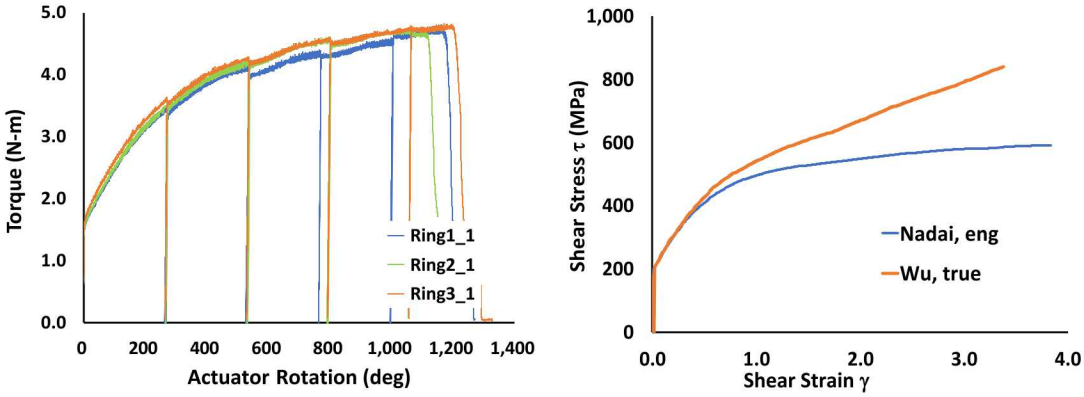

(a) (b)

Figure 4. (a) Torque-rotation and (b) shear stress and strain curves of SS304L-VAR specimens

4. Conclusions

In this work, a new solid bar torsion test is developed. Quantifying shear strains on the order of 2–3 for Al6061-T6 and 3-4 for SS304L are demonstrated. It shows substantial and repeatable strains are achieved up to failure.

For Al6061-T6, localized zone starts to develop at 60% shear strain, and most plastic deformation is developed in the localized zone. The deformation of SS304L specimen is different. It is mainly uniform in the gage section; strain localization only happens very close to failure.

Pure shear stress-strain curves of engineering materials Al6061-T6 and SS304L are obtained. Surface stress evaluation is based on the results of Nadai and Wu. Strains are experimentally measured from the area where strain localization and failure occur.

Sample deformation measurement utilizes 3D DIC method. Several reference configurations need to be employed due to large twist of the cylindrical specimen. DIC analysis for each reference configuration displays incremental deformation, which reveals deformation uniformity or localization.

Strains are calculated from incremental deformation data via repeated exploitation of the multiplicative decomposition of the deformation gradient. The deformation gradient of a surface element of a cylinder under torsion is modeled.

Solid bar torsion provides stable shear deformation and uniform shear stress on the surface of the gage section. Various specimen size could be used depending on torque and DIC capacities. New data are generated for modeling deformation and failure of engineering materials.

Acknowledgement

Sandia National Laboratories is a multimission laboratory managed and operated by National Technology and Engineering Solutions of Sandia, LLC., a wholly owned subsidiary of Honeywell International, Inc., for the U.S. Department of Energy's National Nuclear Security Administration under contract DE-NA-0003525. This talk describes objective technical results and analysis. Any subjective views or opinions that might be expressed in the paper do not necessarily represent the views of the U.S. Department of Energy or the United States Government.

References

[1] Nadai, A., (1950) Theory of Flow and Fracture of Solids, 3rd edition, McGraw-Hill, New York.

[2] Wu, H.C., Xu, Z., and Wang, P.T., (1992) The Shear Stress-Strain Curve Determination from Torsion Test in The Large Strain Range, Journal of Testing and Evaluation, 20: 396–402.

[3] Lyon, R.E., (1991) Shear Strength of a Ductile Material from Torsion of Solid Cylinders, Journal of Testing and Evaluation, 19: 240-243.

[4] Wu, H-C, Xu, Z., and Wang, P.T. (1998) Torsion Test of Aluminum in The Large Strain Range, International Journal of Plasticity, 13: 873-892.

[5] Kingsbury, C.M., May, P.A., Davis, D.A., White, S.R., Moore, J.S., and Sottos, N.R., (2011) Shear Activation of Mechanophore-Crosslinked Polymers, Journal Materials Chemistry, 21: 8381-8388.

[6] Papasidero, J., Doquet, V., and Lepeer, S., (2014) Multiscale Investigation of Ductile Fracture Mechanisms and Strain Localization Under Shear Loading In 2024-T351 Aluminum Alloy and 36 NiCrMo16 Steel, Materials Science & Engineering A, 610: 203–219.